



HAL
open science

Multiple-Input turbo equalization over time-varying frequency selective channel

Christophe Laot, Raphaël Le Bidan, Dominique Leroux

► **To cite this version:**

Christophe Laot, Raphaël Le Bidan, Dominique Leroux. Multiple-Input turbo equalization over time-varying frequency selective channel. EUSIPCO 2002: 11th European Signal Conference, Sep 2002, Toulouse, France. hal-01876231

HAL Id: hal-01876231

<https://hal.science/hal-01876231>

Submitted on 18 Sep 2018

HAL is a multi-disciplinary open access archive for the deposit and dissemination of scientific research documents, whether they are published or not. The documents may come from teaching and research institutions in France or abroad, or from public or private research centers.

L'archive ouverte pluridisciplinaire **HAL**, est destinée au dépôt et à la diffusion de documents scientifiques de niveau recherche, publiés ou non, émanant des établissements d'enseignement et de recherche français ou étrangers, des laboratoires publics ou privés.

Multiple-Input Turbo Equalization Over Time-Varying Frequency Selective Channels

C. Laot, R. Le Bidan and D. Leroux
ENST Bretagne, BP 832, 29285 Brest Cedex, FRANCE

Abstract This paper deals with a low complexity receiver scheme for high order modulation where multiple-input equalization and channel decoding are jointly optimized in an iterative process. Initially proposed in a single-input version the turbo-equalizer is extended for multiple-input. Channel diversity allows performance of the turbo-equalizer to be improved in severe frequency selective environment. Results are presented for 4-QAM and 16-QAM modulations over multipath Rayleigh fading channels.

I. INTRODUCTION

This paper extends the single-input turbo-equalizer [1-2] (SI-TEQ) for multiple receiver antennas allowing channel diversity to be exploited by the equalizer. In turbo-equalization (TEQ), the equalization and channel decoding are jointly optimized. The first version of the TEQ [3] uses a MAP detector to combat ISI. This receiver gives good performance but is essentially dedicated to weak spectral efficiency modulation and short delay spread channels owing to its prohibitive computational complexity. In order to reduce the complexity of the original TEQ, the MAP detector is replaced by an equalizer based on linear filters.

The paper is organized as follows. Section II describes the transmission model. Section III introduces the MI-TEQ structure, which combines a multiple-input equalizer and a SISO decoder. Section IV provides simulation results for MI-TEQ over multipath Rayleigh fading channels, using 4-QAM or 16-QAM. Section V presents our conclusions.

II. PRINCIPLE OF TRANSMISSION SCHEME

Let us consider the transmission scheme depicted in figure 1. A rate R convolutional code is fed in by independent binary data α_k taking the values 0 or 1 with the same probability. A random interleaver is fed in by the coded data $c_{k,i} \in \{\pm 1\}$ and provides interleaved coded data $c_{n,i}$. Each set of $2m$ coded data $c_{n,i}; i=1, \dots, 2m$ is associated with M-ary complex symbol $d_n = (a_n + jb_n)/\sigma$ where symbols a_n and b_n with variance $\sigma^2/2$ take equiprobable values in the set $\{\pm 1, \pm 3, \dots, \pm(\sqrt{M}-1)\}$ with $\sqrt{M} = 2^m$. Symbols d_n with duration T have unitary variance σ_d^2 .

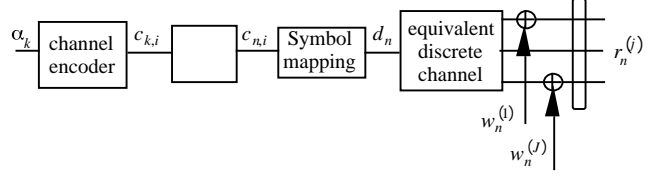


Fig. 1. Transmission scheme

The received signal is modelled by a single-input multiple-output (SIMO) equivalent discrete time channel where each output $j; j=1, \dots, J$ is corrupted by an additive, zero-mean, white Gaussian noise (AWGN) $w_n^{(j)}$ with variance σ_j^2 . The receiver antenna j observes the input $r_n^{(j)}$ equal to

$$r_n^{(j)} = \sum_{l=0}^{L^{(j)}} h_{n,l}^{(j)} d_{n-l} + w_n^{(j)} \quad j=1, \dots, J \quad (1)$$

where $h_{n,l}^{(j)}$ are the $L^{(j)} + 1$ coefficients of the equivalent discrete time channel seen at the antenna j at the time n .

The transfer function of this channel is given by

$$H_n^{(j)}(z) = \sum_{l=0}^{L^{(j)}} h_{n,l}^{(j)} z^{-l} \quad (2)$$

The coefficients of the SIMO channel are supposed normalized to obtain a unitary average power at the input of the receiver

$$\rho_n = \sum_{j=1}^J \sum_{l=0}^{L^{(j)}} |h_{n,l}^{(j)}|^2 \quad \text{with} \quad E\{\rho_n\} = 1 \quad (3)$$

When the noise components $w_n^{(j)}$ are supposed independent, the variance of the noise at the input receiver is equal to

$$\sigma_b^2 = \sum_{j=1}^J \sigma_j^2 \quad (4)$$

The signal to noise ratio (SNR) at the turbo-equalizer input is equal to

$$SNR = \frac{\sigma_d^2}{\sigma_b^2} = R \frac{\bar{E}_b}{N_0} \log_2(M) \quad (5)$$

where \bar{E}_b is the average received energy per information bit, N_0 the one-sided noise power spectral density at the input of the receiver.

III. MULTIPLE-INPUT TURBO-EQUALIZER

For the TEQ, equalization and channel decoding are jointly performed in an iterative way as for a turbo-code [4]. Each iteration p ; $p = 1, \dots, P$ is carried out by a module fed in by both received signal samples $r_n^{(j)}$ and estimated data \bar{d}_n originating from the module $(p-1)$.

As depicted in figure 2, each module consists of an multiple-input equalizer, a symbol to binary converter (SBC), a deinterleaver $^{-1}$, a soft-input soft-output (SISO) binary decoder, an interleaver and a binary to symbol converter (BSC). Each module p delivers an estimate of the symbol d_n , called \bar{d}_n , to be used by the equalizer of the module $p+1$.

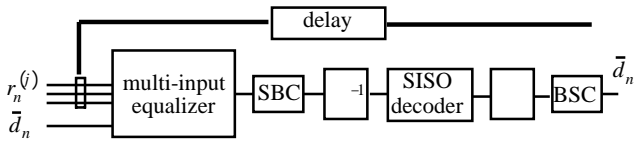


Fig. 2. Structure of the module p

A. Multiple-input equalizer structure

The structure of the equalizer is depicted figure 3. The multiple-input equalizer combines the outputs of the feed forward J transversal filters fed in by the SIMO channel. The intersymbol interference at the combiner output is suppressed by the output of a feedback filter fed in by the estimated symbols \bar{d}_n provided by a previous processing. When the estimated data are equal to the transmitted symbols, this equalizer is a multiple-input Interference Canceller (IC) which allows ISI to be completely removed. The transmitted symbols are generally unknown by the receiver. As a consequence, the equalizer is sub-optimum and it will be necessary to determinate equalizer coefficients for each new symbol received by the TEQ [5].

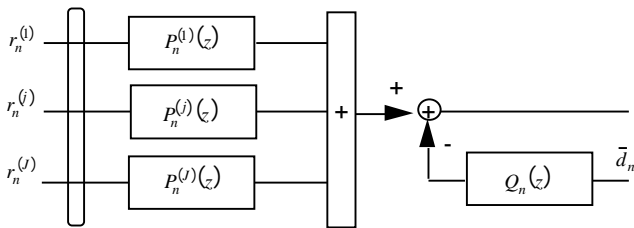


Fig. 3. Multiple-input equalizer

In our approach, in order to simplify the receiver complexity, the equalizer coefficients are calculated under the assumption $\bar{d}_n = d_n$ ($p > 1$). Results presented section V show that when the signal to noise ratio is sufficient, the iterative process gradually increases the reliability of the estimated symbols and the equalizer reaches the performance of the ideal IC.

At the first iteration ($p=1$), the estimated symbols are unknown and supposed equal to zero. According to the mean square error (MSE) criterion, the filter $Q_n(z)$ is equal to zero and the J transversal filters $P_n^{(j)}(z)$ are respectively given by

$$P_n^{(j)}(z) = \frac{H_n^{(j)*}(1/z^*)\sigma_d^2}{\sigma_d^2 \sum_{i=1}^J H_n^{(i)}(z)H_n^{(i)*}(1/z^*) + \sigma_b^2} \quad p=1; j=1, \dots, J \quad (6)$$

For the next iterations ($p > 1$) it is assumed that the symbols \bar{d}_n provide a reliable estimate of d_n . Under the constraint that the central coefficient of the filter $Q_n(z)$ be equal to zero, it can be shown that the multiple-input IC filters have the ideal following transfer function

$$P_n^{(j)}(z) = \frac{\sigma_d^2}{\sigma_d^2 \rho_n + \sigma_b^2} H_n^{(j)*}(1/z^*) \quad p > 1; j=1, \dots, J \quad (7)$$

$$Q_n(z) = \frac{\sigma_d^2 \rho_n}{\sigma_d^2 \rho_n + \sigma_b^2} \sum_{i=1}^J H_n^{(i)}(z)H_n^{(i)*}(1/z^*) - \rho_n \quad p > 1 \quad (8)$$

Thus, the IC output is ISI free and equal to

$$s_n = \frac{\sigma_d^2}{\sigma_d^2 \rho_n + \sigma_b^2} \rho_n d_n + \sum_{j=1}^J h_{n,j}^{(j)*} w_{n+j}^{(j)} \quad (9)$$

From (9) it can be proved that the signal to noise ratio at the multiple-input IC output is equal to (5). Thus, it clearly appears that ISI is completely removed by the equalizer and the energy of the different filter taps is collected without noise enhancement.

B. Symbol to Binary Converter (SBC)

The function SBC permits the use of a single decoder whatever the states number of the M-QAM modulation. The symbol to binary converter associates values $eq(c_{n,i})$, representative of $2m$ binary coded data $c_{n,i}$; $i=1, 2, \dots, 2m$, to each sample $s_n = u_n + jv_n$ provided by the equalizer. Values $eq(c_{n,i})$ are defined as the log likelihood ratio (LLR) of binary coded data conditionally to the observation u_n (resp. v_n) representative of symbol a_n (resp. b_n).

$$eq(c_{n,i}) = \log \frac{\Pr\{c_{n,i} = 1/u_n\}}{\Pr\{c_{n,i} = -1/u_n\}} \quad i = 1, \dots, m \quad (10)$$

$$eq(c_{n,i}) = \log \frac{\Pr\{c_{n,i} = 1/v_n\}}{\Pr\{c_{n,i} = -1/v_n\}} \quad i = m+1, \dots, 2m$$

A symbol a_n is a representative form of a binary coded data vector, with dimension m , such that $\mathbf{c}_n = (c_{n,1}, \dots, c_{n,i}, \dots, c_{n,m})$. Let us denote $a_n(\mathbf{c}_n)$ the symbol a_n associated with one among 2^m possible realizations of

\mathbf{c}_n . Considering $c_{ni} = \lambda$; $\lambda = 0, 1$, we define a new vector $\mathbf{c}_n: c_{ni} = \lambda$ that has 2^{m-1} possible realizations. By applying Bayes' rule, the LLR given by the relation (10) may be rewritten as

$$eq(c_{ni}) = \log \frac{p\{u_n/\mathbf{c}_n\}_{\mathbf{c}_n: c_{ni}=1}}{p\{u_n/\mathbf{c}_n\}_{\mathbf{c}_n: c_{ni}=-1}} \quad i = 1, \dots, m \quad (11)$$

where $p\{u_n/\mathbf{c}_n\}$ is the probability density function (pdf) of observation u_n conditionally to the transmitted symbol $a_n(\mathbf{c}_n)$. This pdf follows a Gaussian law $N(\mu_n a_n(\mathbf{c}_n), \sigma_n^2)$ according to relation (9) and the LLR may be expressed as

$$eq(c_{ni}) = \log \frac{\exp\left(-\frac{(u_n - \mu_n a_n(\mathbf{c}_n))^2}{2\sigma_n^2}\right)_{\mathbf{c}_n: c_{ni}=1}}{\exp\left(-\frac{(u_n - \mu_n a_n(\mathbf{c}_n))^2}{2\sigma_n^2}\right)_{\mathbf{c}_n: c_{ni}=-1}} \quad (12)$$

C. SISO channel decoder

The channel decoder is a SISO (Soft Input Soft Output) device which implements the BCJR-MAP algorithm [6]. The observations provided by the SBC, called *obs*, fed the channel decoder input which delivers soft output decisions on coded data

$$dec(c_{k,i}) = \log \frac{\Pr\{c_{k,i} = 1/obs\}}{\Pr\{c_{k,i} = -1/obs\}} \quad (13)$$

This LLR fed the binary to symbol converter in order to provide an estimated symbols.

D. Binary to Symbol Converter (BSC)

To feed the equalizer filter $Q_n(f)$ it is necessary for the transmitted symbols to be known or estimated. When transmitted symbols are unknown, it is possible to get an estimated value $\bar{d}_n = (\bar{a}_n + j\bar{b}_n)/\sigma$ from the LLRs on coded data provided by the channel decoder of the previous module. This paragraph proposes a solution to produce an M-ary symbol from the binary decoder soft output.

As previously, $a_n(\mathbf{c}_n)$ denotes the symbol a_n associated with one among 2^m possible realizations of \mathbf{c}_n . Then, estimate \bar{a}_n of a_n may be approximated by its conditional expected value

$$\bar{a}_n = E\{a_n(\mathbf{c}_n)/obs\} \quad (14)$$

Owing to (13), it can be shown that

$$E\{c_{n,l}/obs\} = \tanh\left(\frac{dec(c_{n,l})}{2}\right) \quad (15)$$

Using a Gray coding defined by the following relations

$$\begin{aligned} a_n(\mathbf{c}_n) &= c_{n1} & M &= 4 \\ a_n(\mathbf{c}_n) &= c_{n1} \cdot (2 + c_{n2}) & M &= 16 \end{aligned} \quad (16)$$

Then, estimated symbols of the expression (14) are given by

$$\begin{aligned} \bar{a}_n &= \tanh\left(\frac{dec(c_{n,1})}{2}\right) & M &= 4 \\ \bar{a}_n &= \tanh\left(\frac{dec(c_{n,1})}{2}\right) \cdot \left(2 + \tanh\left(\frac{dec(c_{n,2})}{2}\right)\right) & M &= 16 \end{aligned} \quad (17)$$

\bar{b}_n can be obtained using a similar derivation.

IV. SIMULATION RESULTS

Radiocommunication propagation is generally subject to multipaths corrupted by Doppler effects, which depend on the relative speed between emitter and receiver and also on the carrier frequency. The taps coefficients of each equivalent discrete channel seen by the antenna j ; $j = 1, \dots, J$ can be modelled by a complex-valued independent random process, which may be expressed as

$$h_{n,l}^{(j)} = \sqrt{\frac{P_l^{(j)}}{N}} \exp\left\{j\left(2\pi f_d \cos \xi_{l,i}^{(j)} nT + \psi_{l,i}^{(j)}\right)\right\} \quad (18)$$

where f_d and $P_l^{(j)}$ denote respectively the maximum Doppler frequency spread and the average power associated with the l -th path. Parameters $\xi_{l,i}^{(j)}$ and $\psi_{l,i}^{(j)}$ are uniform random variables over $[0; 2\pi]$. For simulations we have chosen $N = 10$. The Doppler effect is characterized by the product of the Doppler band $B_d = 2f_d$ by T . The vector $\mathbf{P}^{(j)}$ collects the average powers associated to the coefficients of the multiple-output discrete equivalent channels used for simulations. Notice that all the antennas receive equal average power

$$\mathbf{P}^{(j)} = \left[P_0^{(j)} \dots P_l^{(j)} \dots P_{L^{(j)}+1}^{(j)} \right] / J; j = 1, \dots, J \quad (19)$$

For simulations, the information data were coded using a rate 1/2 convolutional code with octal generator polynomials 23,35. A 128x128 random matrix performed the interleaving. In order to evaluate the asymptotic performance of the proposed scheme, the channel taps and noise variance were assumed to be known at the receiver side.

In the figures, we have represented by a dashed line the bound of the turbo-equalizer, which corresponds to the ideal situation of the IC fed in by the known transmitted symbols. The turbo-equalization goal is to reach this bound. At the IC output, ISI is completely cancelled and the energy from the different channel taps is collected. This explains the diversity gain in comparison with the Rayleigh non-frequency selective channel (EQ1) plotted by a dash-dot line. For reference purpose, we have plotted with a dotted line the receiver performance over a Gaussian non-selective channel.

Results presented in figure 4 are given for the SI-TEQ over a Rayleigh discrete equivalent channel with $B_d T = 0.01$ and three paths with equal average power.

$$\text{EQ3} \quad \mathbf{P}^{(1)} = [1/3 \ 1/3 \ 1/3]$$

Performance of SI-TEQ is plotted in solid line (4 iterations). After three iterations, the SI-TEQ converges towards the bound as the signal to noise ratio becomes greater than 3 dB.

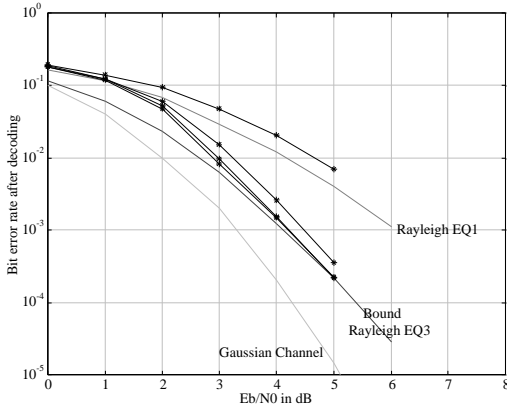


Fig. 4. Performance of the SI-TEQ with 4-QAM over the EQ3 Rayleigh channel

Performance presented in figure 5 are given for the MI-TEQ over a three-output channel with $B_d T = 0.01$, using 4-QAM. Each antenna received a three paths Rayleigh channel.

$$\text{3EQ3} \quad \mathbf{P}^{(j)} = [1/3 \ 1/3 \ 1/3]/3 \quad ; j = 1,2,3$$

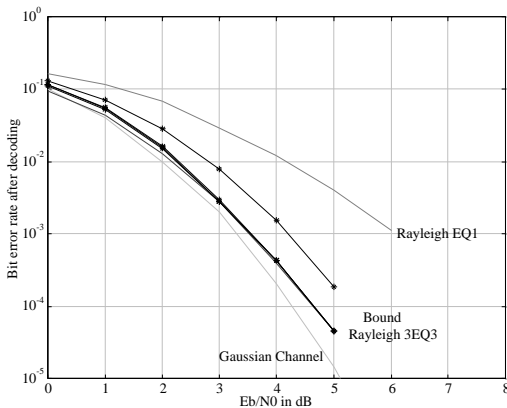


Fig. 5. Performance of the MI-TEQ with 4-QAM for three antennas and 3EQ3 Rayleigh channel

Performance of MI-TEQ is plotted in solid line (4 iterations). After only two iterations, performance of the MI-TEQ reaches the IC bound. Diversity of the transmission allows MI-TEQ performance to approach closely the Gaussian non selective channel performance even for low signal to noise ratio.

In figure 6 we investigate the performance of the MI-TEQ for 16-QAM over the multiple-output channel 3EQ3. Performance of MI-TEQ is plotted in solid line (4 iterations). After only three iterations, performance of the MI-TEQ reaches the IC bound.

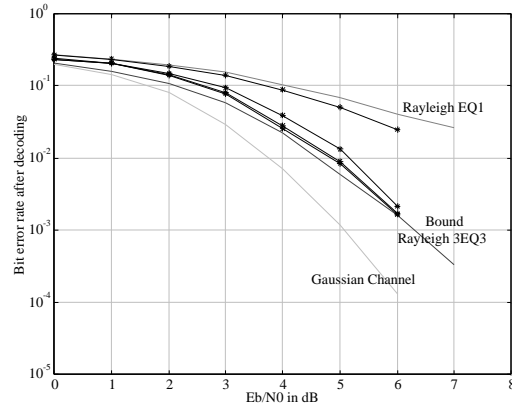


Fig. 6. Performance of the MI-TEQ with 16-QAM for three antennas and 3EQ3 Rayleigh channel

We would like to emphasize the low complexity of this receiver in comparison with classical MAP receiver. Indeed, using a MAP detector to equalize HT100 channel with 16-QAM modulation requires a trellis with more than 10^6 states whereas the MI-TEQ needs only linear filtering with a limited number of coefficients to perform equalization.

V. CONCLUSION

This paper describes a low complexity multiple-input receiver for high order modulations and large delay spread channels. After only few iterations, the MI-TEQ removes ISI, collects the energy of the different taps and exploits the coding gain. Presented in this paper with 4-QAM and 16-QAM, the MI-TEQ can be easily extended to higher order modulation without increasing the complexity.

REFERENCES

- [1] A. Glavieux, C. Laot and J. Labat, "Turbo-equalization over a frequency selective channel," *Symposium on Turbo-Codes*, pp. 96-102, Brest, Septembre 1997.
- [2] C. Laot et al, "Turbo Equalization : Adaptive Equalization and Channel Decoding Jointly Optimized," *IEEE JSAC*, VOL. 29, NO. 9, september 2001.
- [3] C. Douillard et al., "Iterative Correction of Intersymbol Interference : Turbo-equalization", *European Transactions on Telecommunications*, Vol.6, N°5, pp. 507-511, 1995.
- [4] C. Berrou and A. Glavieux, " Near Optimum Error Correcting Coding And Decoding : Turbo-codes," *IEEE Trans. Comm.* Vol. 44, N°10, pp.1262-1271, Oct. 1996.
- [5] M. Tüchler et al "Turbo Equalization: principles and new results," submitted to the *IEEE Trans. on Com.*, August, 2000. Preprint, <http://www.uiuc.edu/~acsinger/>
- [6] L.R. Bahl et al., "Optimal Decoding of Linear Codes for Minimizing Symbol Error Rate", *IEEE Trans. Info. Theory*, Vol IT-20, no. 3, pp. 284-287, March 1974.